Available online at www.sciencedirect.com
ScienceDirect
Trans. Nonferrous Met. Soc. China 29(2019) 1332−1345
Transactions of Nonferrous Metals Society of China
www.tnmsc.cn

Kinetics of celestite conversion to acidic strontium oxalate hydrate in aqueous solution of oxalic acid

Mert ZORAGA, Cem KAHRUMAN, Ibrahim YUSUFOGLU

Istanbul University-Cerrahpasa, Engineering Faculty,
Metallurgical and Materials Engineering Department, 34320, Avcilar, Istanbul, Turkey

Received 7 September 2018; accepted 29 December 2018

Abstract: Conversion of $SrSO_4$ to acidic strontium oxalate hydrate ($H[Sr(C_2O_4)_{1.5}(H_2O)]$) in aqueous $H_2C_2O_4$ solutions proceeds as a consecutive reaction. In the first step of the consecutive reaction, $SrSO_4$ reacts with $H_2C_2O_4$ and pseudomorphic conversion to $SrC_2O_4·H_2O$ occurs. In the second step, $SrC_2O_4·H_2O$ reacts with $H_2C_2O_4$ to form $H[Sr(C_2O_4)_{1.5}(H_2O)]$. $Sr(HC_2O_4)(C_2O_4)_{0.5}·H_2O$ crystallizes during cooling of the reaction mixture to room temperature if the solution reaches the saturation concentration of $H[Sr(C_2O_4)_{1.5}(H_2O)]$. The aims of this study are the derivation of reaction rate equations and the determination of the kinetic parameters such as pre-exponential factor, apparent activation energy and order of $H_2C_2O_4$ concentration for each reaction step. Fractional conversions of $SrSO_4$ were calculated using the quantitative amounts of dissolved S and Sr. It was determined that the reaction rate increased at the initial time of reaction by increasing the temperature using solutions with approximately same $H_2C_2O_4$ concentrations. The reaction extends very slowly after a certain time in solutions with low $H_2C_2O_4$ concentration and ends by the formation of a protective layer of $SrC_2O_4·H_2O$ around the surfaces of solid particles. Fractional conversion of $SrSO_4$ is increased by increasing concentration of $H_2C_2O_4$ at constant temperature. Kinetic model equations were derived using shrinking core model for each step.

Key words: celestite concentrate; pseudomorphic conversion; rate equations; kinetic parameters; conversion reaction

1 Introduction

Celestite ($SrSO_4$) and strontianite ($SrCO_3$) are minerals used commonly for industrial purposes. Celestite is converted in industrial applications firstly to $SrCO_3$ by pyrometallurgical, hydrometallurgical or mechanochemical methods and then it is converted to other compounds such as $SrCl_2$, $SrCrO_4$, $Sr(NO_3)_2$ and SrO. There are two commonly used $SrCO_3$ production processes: black ash and direct conversion. In the black ash process, $SrSO_4$ is reduced with coke to produce water soluble SrS and the SrS is leached with water and finally reacted either with Na_2CO_3, CO_2 or other carbonating agent solutions [1−3]. Metallothermic method by using Al or Mg as reductant was applied for the reduction of celestite to SrS [4,5]. In the direct conversion process, concentrated celestite reacts with CO_3^{2-} ion-containing solutions to form the insoluble $SrCO_3$ at low temperatures [6−10]. Mechanochemical method is applied for the conversion of celestite to $SrCO_3$ [11−15].

Strontium oxalate is a precursor for the production of strontium compounds such as Bi−Sr−Ca−Cu−O (BSCCO) high-temperature superconductive materials. It must be pure, homogeneous and has a definite composition [16]. BSCCO materials were produced by co-precipitation from their nitrate solutions using $H_2C_2O_4$ and $(NH_4)_2C_2O_4$ solutions. The production of superconductive metal oxide materials by thermal decomposition of co-precipitated or mechanically-mixed metal oxalates was also investigated [16−18].

Two types of strontium oxalate hydrates have been known: neutral ($SrC_2O_4·xH_2O$, x=1, 1.25, 2 and 2.5) and acidic ($Sr(HC_2O_4)(C_2O_4)_{0.5}·H_2O$ or $SrC_2O_4(H_2C_2O_4)_{0.5}·H_2O$). The production of neutral or acidic strontium oxalates depends on oxalate reactant used ($H_2C_2O_4$ or $(NH_4)_2C_2O_4$), pH, temperature of the solution and drying time of the precipitate. XRD and neutron diffraction techniques were used for the structural investigation of acidic strontium oxalate [18]. Dumbbell-shaped, peanut-shaped, transparent prismatic bi-pyramidal platy-shaped

Corresponding author: Mert ZORAGA; Tel: +90-212-4737070/17649; Fax: +90-212-4737180; E-mail: mzoraga@istanbul.edu.tr
DOI: 10.1016/S1003-6326(19)65040-5

and spherulite type single crystal strontium oxalates were also prepared [19−21].

The effects of $H_2C_2O_4$, $Na_2C_2O_4$ and $(NH_4)_2C_2O_4$ solutions on the conversion of reagent grade $SrSO_4$ and celestite mineral to strontium oxalate hydrate were investigated by XRD and it was found that aqueous $H_2C_2O_4$ and $Na_2C_2O_4$ solutions had no or little effect on reagent grade $SrSO_4$ or celestite concentrate, but aqueous $(NH_4)_2C_2O_4$ solution converted them into $SrC_2O_4·H_2O$ [22]. BACCE et al [23] investigated the precipitation of $SrC_2O_4·H_2O$ by mixing $SrCl_2$ and $(NH_4)_2C_2O_4$ solutions under conventional and ultrasonic stirring conditions. $SrC_2O_4·H_2O$ and SrC_2O_4 particles have been obtained in ellipsoid shape using these experimental conditions.

The investigation of the thermal decomposition mechanism of neutral oxalate hydrate ($SrC_2O_4·xH_2O$, where x=1, 1.25, 2 or 2.5) was performed under different gas atmospheres such as air, H_2, N_2 and CO_2 [17,24−26]. KNAEPAN et al [16] investigated the thermal decomposition behavior of co-precipitated $Ca_xSr_{1-x}C_2O_4$, mechanically-mixed SrC_2O_4 and CaC_2O_4 and acidic strontium oxalate hydrate.

There is no study in literature that examined systematically the conversion mechanism of celestite to acidic strontium oxalate hydrate. Therefore, we focused on this subject in our previous work [27] at which we have determined the conversion mechanism of celestite to acidic strontium oxalate and characterized the by- and end-products obtained during the conversion reaction using excess amounts of $H_2C_2O_4$ with respect to the conversion reaction stoichiometry. We used XRD, ICP−OES and simultaneous TGA−DTA−MS analytical techniques to explain the conversion mechanism of $SrSO_4$ to acidic strontium oxalate hydrate.

We determined that the conversion of $SrSO_4$ to acidic strontium oxalate in aqueous $H_2C_2O_4$ solutions proceeds in two consecutive reaction steps: In the first step of the consecutive reaction, the conversion of $SrSO_4$ to $SrC_2O_4·H_2O$ is a solid−liquid heterogeneous type reaction. The solubility products of $SrSO_4$ and $SrC_2O_4·H_2O$ are $K_{Sp,SrSO_4}=2.8\times10^{-7}$ and $K_{Sp,SrC_2O_4·H_2O}=5\times10^{-8}$, respectively [2,21]. This indicates that the solubility of $SrC_2O_4·H_2O$ is lower than $SrSO_4$. As a result of the difference in the solubility of these solid substances, a driving force is generated for the realization of the solid−liquid heterogeneous type reaction. The first step of the consecutive reaction proceeds by the exchange of SO_4^{2-} ions with the $C_2O_4^{2-}$ ions present in the bulk solution. The naturally occurred $SrSO_4$ particles are non-porous. The molar volume of $SrC_2O_4·H_2O$ (71.18×10^{-3} m^3/kmol) is 53.47% greater than the molar volume of $SrSO_4$ (46.38×10^{-3} m^3/kmol) [15]. Therefore, $SrC_2O_4·H_2O$ layer formed around the $SrSO_4$ particles during the pseudomorphic conversion must have a protective layer. This protective layer of the $SrC_2O_4·H_2O$ hinders the collision of solid reactant surfaces with $H_2C_2O_4$ in the liquid bulk phase. Therefore, ion-exchange reaction between $SrSO_4$ and $H_2C_2O_4$ proceeds up to the covering of the $SrSO_4$ particle surfaces with the protective layer of $SrC_2O_4·H_2O$. The conversion reaction proceeds because the protective layer reacts with $H_2C_2O_4$ during the second step of the consecutive reaction and again the surfaces of the $SrSO_4$ reactant particles are free and ready for contact with $H_2C_2O_4$.

In the second step of the consecutive reaction, $SrC_2O_4·H_2O$ formed during the first step reacts with $H_2C_2O_4$ to form the water soluble $H[Sr(C_2O_4)_{1.5}(H_2O)]$ which undergoes the bulk solution phase. This explanation was made due to the concentration of strontium in solution determined by quantitative chemical analysis of ICP−OES is much more than the concentration of strontium that can be come from the dissolution of $SrC_2O_4·H_2O$. The conversion reaction proceeds up to the saturation concentration of $H[Sr(C_2O_4)_{1.5}(H_2O)]$. By reaching the saturation concentration of $H[Sr(C_2O_4)_{1.5}(H_2O)]$, the second step of the consecutive reaction stops while $SrC_2O_4·H_2O$ formed on the surfaces of the reactant $SrSO_4$ particles can not be removed. At the end of experiment, by decreasing the temperature to room temperature, $Sr(HC_2O_4)(C_2O_4)_{0.5}·H_2O$ crystallizes if its concentration in the solution is higher than its saturation concentration at room temperature.

The aims of this study were the derivation of reaction rate equations for each reaction step of $SrSO_4$ conversion and the determination of the kinetic parameters such as pre-exponential factor, apparent activation energy and order of $H_2C_2O_4$ concentration. The effects of stirring speed, celestite particle size, $H_2C_2O_4$ concentration and temperature on the conversion reaction rate were also investigated. Fractional conversion versus time curves drawn by using the derived Kinetic Model Equations were compared to the experimental findings.

2 Experimental

2.1 Celestite concentrate

Celestite concentrate was provided by Barit Maden Turk A.S.. The celestite concentrate was wet sieved (Octagon 200) to obtain four particle size fractions: 250−315, 150−180, 90−125 and 38−45 μm. The fractions were dried in oven (Binder ED 115) at 378 K for 8 h. Phase and chemical composition of celestite concentrate were determined by XRD, Rietveld (Rigaku D/Max−2200) and XRF (Panalytical Axios−Minerals) analytical methods. 2 g of celestite concentrate was used

in each experiment.

2.2 Oxalic acid solutions

0.1, 0.2, 0.4, 0.8 and 1.2 mol of $H_2C_2O_4$ was dissolved in 1 L solution. The exact concentration of $H_2C_2O_4$ in the prepared solution was determined by volumetric analysis (titration) using 0.1 mol/L standard $KMnO_4$ solution (Merck) [28]. 1 L solution was used in each experiment.

2.3 Experimental set-up

Experiments were performed in a hydro-metallurgical glass reactor with total volume of 1.5 L (HWS). Isothermal condition in the reactor was achieved by continuous circulation of hot water through the jacket of the reactor and by mechanical stirring of the reactor content. Circulation of water at constant temperature was provided from a thermostatic bath (Julabo). When isothermal conditions were obtained in the reactor, celestite concentrate was added to the reactor. The conversion reaction of $SrSO_4$ was carried out under isothermal conditions at temperatures of 301.5, 313, 328, 343 and 358 K and stirring speeds of 300, 400 and 500 r/min. A special sampling apparatus with a porous ceramic disc at the end of a glass tube was used to take solutions without solid contamination. 10 mL solution samples were taken from the reactor at certain time intervals for quantitative analysis of S (coming from HSO_4^- ions) and Sr (coming from strontium chelate compound) that are present in the solution. Equal volume of fresh acid solution was added to the reactor after each sampling in order to maintain the reactor volume and $H_2C_2O_4$ concentration approximately constant during conversion reaction. Quantitative analyses of dissolved elements in the solution samples were carried out by ICP−OES instrument (Spectro Ciros Vision).

3 Results and discussion

3.1 Characterization of celestite concentrate

XRF and Rietveld quantitative analysis results of four particle size fractions of celestite concentrate (Table 1) indicated that all size fractions included main compound $SrSO_4$ and major contaminations $CaCO_3$, $BaSO_4$, SiO_2, Fe_2O_3, Al_2O_3 and $PbSO_4$. The amounts (<0.05 wt.%) of minor contaminations of celestite concentrate (CuO, ZnO and NiO) were not shown in Table 1. XRD patterns of the celestite concentrates (XRD pattern of the celestite concentrate with particle size fraction of 90−125 μm was given in our previous study [27]) came only from the peaks of $SrSO_4$ (ICDD 05-0593) while the peaks of the major contaminations are not detectable since their amounts in celestite concentrate are too low.

Table 1 Chemical composition of various particle size fractions of celestite concentrate

Compound	Composition/wt.%			
	250−315 μm	150−180 μm	90−125 μm	38−45 μm
$SrSO_4$	95.506	93.888	95.738	93.640
$CaCO_3$	2.395	3.639	2.151	3.390
$BaSO_4$	1.109	1.292	1.414	1.680
SiO_2	0.559	0.687	0.318	0.693
Fe_2O_3	0.272	0.283	0.191	0.353
Al_2O_3	0.063	0.097	0.078	0.118
$PbSO_4$	0.066	0.059	0.064	0.079

3.2 Dissolution behavior of $H_2C_2O_4$

$H_2C_2O_4$ is a diprotic acid. Therefore, Reactions (1) and (2) occur as a consecutive reaction during the dissolution of $H_2C_2O_4$ in water. The temperature dependency of acid dissociation constants of Reactions (1) (K_1) and 2 (K_2) is given, where pK is defined as $-\lg K$ [29,30]. K_1 and K_2 were calculated for each temperature according to Eqs. (1) and (2) (Table 2):

$$H_2C_2O_4(d) \rightleftharpoons HC_2O_4^-(aq) + H^+(aq), \quad pK_1 = 1.953 - 203.686/T \tag{1}$$

$$HC_2O_4^-(aq) \rightleftharpoons C_2O_4^{2-}(aq) + H^+(aq), \quad pK_2 = 5.492 - 365.59/T \tag{2}$$

Table 2 Acid dissociation constants of Reactions (1) and (2) at various temperatures

T/K	K_1	K_2
301.5	5.279×10^{-2}	5.255×10^{-5}
313	4.986×10^{-2}	4.743×10^{-5}
328	4.656×10^{-2}	4.194×10^{-5}
343	4.373×10^{-2}	3.748×10^{-5}
358	4.135×10^{-2}	3.382×10^{-5}

Concentrations of $C_2O_4^{2-}$, $HC_2O_4^-$, $H_2C_2O_4$ and H^+ are calculated by solving two equations with two variables obtained using K_1 and K_2 values given in Table 2 for each temperature and the amounts of $H_2C_2O_4$ used for the preparation of 1 L solution. The calculated values of $C_2O_4^{2-}$, $HC_2O_4^-$, $H_2C_2O_4$ and H^+ concentrations are given in Table 3. It was observed that the amounts of $C_2O_4^{2-}$ group containing molecules given in Table 3 are in good agreement with the volumetric analysis results.

Enthalpies of Reactions (1) and (2) were calculated for each temperature according to pK_1 and pK_2 as −3.9 and −7 kJ/mol, indicating that both reactions are exothermic. When the amount of $H_2C_2O_4$ used for the preparation of 1 L solution is kept constant and the temperature of the solution increases, $H_2C_2O_4$ concentration increases and $C_2O_4^{2-}$, $HC_2O_4^-$ and H^+

Table 3 Concentrations of $C_2O_4^{2-}$, $HC_2O_4^-$, $H_2C_2O_4$ and H^+ obtained by dissolving various amounts of $H_2C_2O_4$ in 1 L solution

T/K	$C_2O_4^{2-}$ concentration/(mol·L^{-1})				
	$c(H_2C_2O_4)$=0.10 mol/L	$c(H_2C_2O_4)$=0.20 mol/L	$c(H_2C_2O_4)$=0.40 mol/L	$c(H_2C_2O_4)$=0.80 mol/L	$c(H_2C_2O_4)$=1.20 mol/L
301.5	5.2442×10^{-5}	5.2481×10^{-5}	5.2505×10^{-5}	5.2519×10^{-5}	5.2526×10^{-5}
313	4.7340×10^{-5}	4.7372×10^{-5}	4.7392×10^{-5}	4.7404×10^{-5}	4.7410×10^{-5}
328	4.1868×10^{-5}	4.1894×10^{-5}	4.1909×10^{-5}	4.1919×10^{-5}	4.1924×10^{-5}
343	3.7421×10^{-5}	3.7442×10^{-5}	3.7455×10^{-5}	3.7463×10^{-5}	3.7467×10^{-5}
358	3.3771×10^{-5}	3.3789×10^{-5}	3.3799×10^{-5}	3.3806×10^{-5}	3.3809×10^{-5}
T/K	$HC_2O_4^-$ concentration/(mol·L^{-1})				
	$c(H_2C_2O_4)$=0.10 mol/L	$c(H_2C_2O_4)$=0.20 mol/L	$c(H_2C_2O_4)$=0.40 mol/L	$c(H_2C_2O_4)$=0.80 mol/L	$c(H_2C_2O_4)$=1.20 mol/L
301.5	0.050855	0.079641	0.121244	0.180745	0.226623
313	0.049906	0.077947	0.118429	0.176292	0.220895
328	0.048775	0.075945	0.115119	0.171074	0.214194
343	0.047747	0.074140	0.112150	0.166411	0.208215
358	0.046837	0.072551	0.109550	0.162342	0.203004
T/K	$H_2C_2O_4$ concentration/(mol·L^{-1})				
	$c(H_2C_2O_4)$=0.10 mol/L	$c(H_2C_2O_4)$=0.20 mol/L	$c(H_2C_2O_4)$=0.40 mol/L	$c(H_2C_2O_4)$=0.80 mol/L	$c(H_2C_2O_4)$=1.20 mol/L
301.5	0.049092	0.120307	0.278704	0.619203	0.973324
313	0.050047	0.122005	0.281523	0.623660	0.979057
328	0.051183	0.124013	0.284839	0.628884	0.985764
343	0.052215	0.125823	0.287812	0.633551	0.991747
358	0.053120	0.127415	0.290416	0.637625	0.996962
T/K	H^+ concentration/(mol·L^{-1})				
	$c(H_2C_2O_4)$=0.10 mol/L	$c(H_2C_2O_4)$=0.20 mol/L	$c(H_2C_2O_4)$=0.40 mol/L	$c(H_2C_2O_4)$=0.80 mol/L	$c(H_2C_2O_4)$=1.20 mol/L
301.5	0.050960	0.079746	0.121348	0.180850	0.226728
313	0.050001	0.078042	0.118524	0.176387	0.220990
328	0.048859	0.076029	0.115203	0.171158	0.214278
343	0.047822	0.074177	0.112225	0.166486	0.208290
358	0.046905	0.072619	0.109618	0.162409	0.203072

ion concentrations decrease in accordance with the Le Chatelier's Principle. On the other hand, when the temperature of the solution is kept constant and the amount of $H_2C_2O_4$ used for the preparation of 1 L solution increases, H^+, $HC_2O_4^-$ and $H_2C_2O_4$ concentrations increase and the concentration of $C_2O_4^{2-}$ remains approximately constant (Table 3).

3.3 Calculation of fractional conversion

Fractional conversions of $SrSO_4$ were calculated using ICP−OES (Spectro Ciros Vision) quantitative chemical analysis results of S and Sr present in the solutions taken during the conversion experiments at certain time intervals. Fractional conversion of $SrSO_4$ was calculated according to Eq. (3):

$$X_i = \frac{W_i}{W_{i,0}} \tag{3}$$

where X_i (i: S or Sr) is the fractional conversion of $SrSO_4$, $W_{i,0}$ is the initial mole amount of i elements and W_i is the mole amount of i elements of reacted $SrSO_4$ to produce soluble HSO_4^- or soluble strontium chelate molecules at any reaction time.

Normally, X_{Sr} and X_S values must be equal if all reacted $SrSO_4$ produces equimolar amounts of water soluble HSO_4^- ions and water soluble strontium chelate molecules. It was determined in all experiments that $X_{Sr}<X_S$. This result indicates clearly that a part of the reacted $SrSO_4$ was converted to insoluble strontium oxalate hydrate during the conversion reaction of $SrSO_4$.

3.4 Effect of stirring speed on conversion reaction rate of $SrSO_4$

The effect of stirring speed on the conversion reaction rate of $SrSO_4$ was investigated using 300, 400 and 500 r/min, 2 g of celestite concentrate with particle size fraction of 90−125 μm, 1 L solution obtained by dissolving 1.20 mol $H_2C_2O_4$ and 358 K (Fig. (1)). It can be seen that increase of stirring speed from 300 to 500 r/min has no effect on the conversion reaction rate.

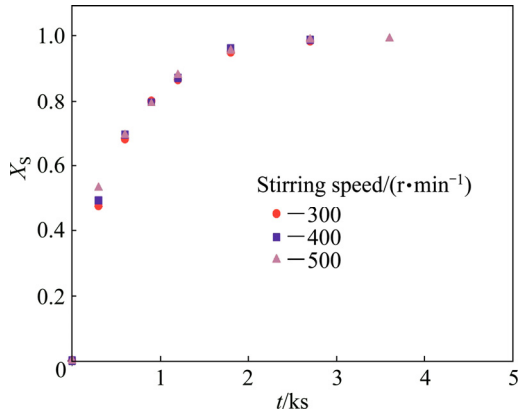

Fig. 1 X_S vs t diagrams for various stirring speeds (celestite: 0.0104 mol, particle size: 90−125 μm, solution: 1 L, $H_2C_2O_4$: 1.2 mol, temperature: 358 K)

Therefore, the resistance of the liquid film layer that surrounds the surfaces of celestite particles is not effective on the conversion reaction rate by using stirring speed of 500 r/min. This stirring speed was kept constant at all experiments where effects of other kinetic parameters affecting reaction rate were investigated.

3.5 Effect of $H_2C_2O_4$ concentration and temperature on conversion reaction rate of $SrSO_4$

X_S vs t and X_{Sr} vs t diagrams obtained for 301.5, 313, 328, 343 and 358 K and 1 L solutions obtained by dissolving 0.1, 0.2, 04, 0.8 and 1.2 mol $H_2C_2O_4$ are shown in Fig. 2. The diagrams in Figs. 2(a−e) show the effect of $H_2C_2O_4$ concentration on the conversion reaction rate of $SrSO_4$ at constant temperature. While the same amount of $H_2C_2O_4$ was used for each temperature,

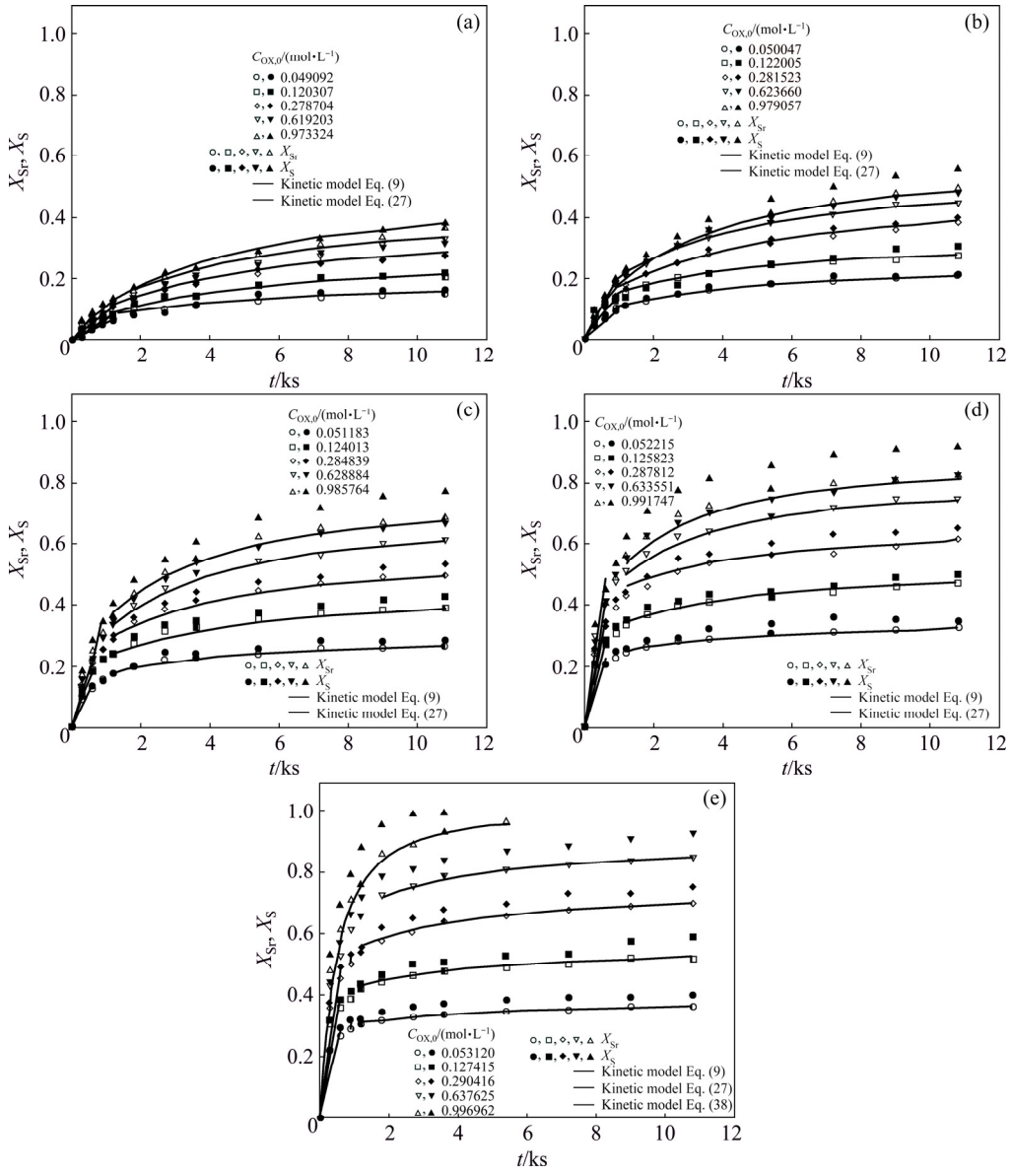

Fig. 2 X_S vs t and X_{Sr} vs t diagrams for various $H_2C_2O_4$ concentrations and temperatures (celestite: 0.0104 mol, particle size: 90−125 μm, solution: 1 L, stirring speed: 500 r/min): (a) 301.5 K; (b) 313 K; (c) 328 K; (d) 343 K; (e) 358 K

amounts of $H_2C_2O_4$ in 1 L solutions were not the same because of equilibrium Reactions (1) and (2). Therefore, real amounts of $H_2C_2O_4$ in 1 L solutions are the concentrations given in Table 3 and these values were used in the calculation of reaction rate parameters.

The X_S vs t diagrams given in Fig. 3 show the effect of temperature on the conversion reaction rate of $SrSO_4$ at constant dissolved amount of $H_2C_2O_4$ (1.2 mol) in 1 L solution. Diagrams obtained for other constant dissolved amounts of $H_2C_2O_4$ in 1 L solution at various temperatures were not shown to avoid repetition.

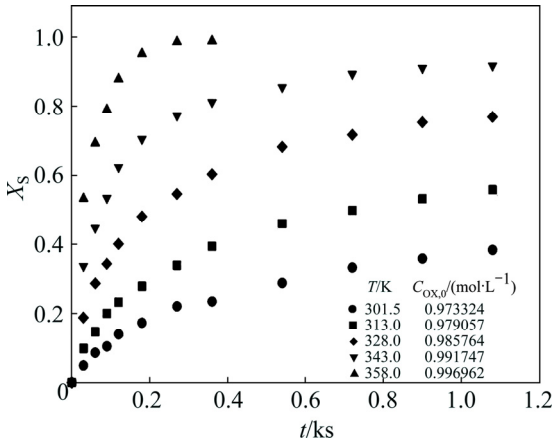

Fig. 3 X_S vs t diagrams for various temperatures (celestite: 0.0104 mol, particle size: 90−125 μm, solution: 1 L, stirring speed: 500 r/min)

X_S vs t and X_{Sr} vs t diagrams in Figs. 2(a−e) show that in the initial stage of conversion reaction, increase of $H_2C_2O_4$ concentration at constant temperature increased the conversion rate of $SrSO_4$. This indicated that the concentration of $H_2C_2O_4$ has a distinct effect on the conversion reaction rate and therefore its order must be introduced in rate equation. The increase of temperature from 301.5 to 358 K in solutions that have approximately the same concentration of $H_2C_2O_4$ (Figs. 2(a−e) and Fig. 3) increased the conversion reaction rate effectively at the initial stage of reaction. This indicated that the reaction is under chemical reaction kinetics control. Conversion reaction rate decreases progressively after a certain period of reaction at constant temperature and $H_2C_2O_4$ concentration.

3.6 Effect of celestite particle size on conversion reaction rate of $SrSO_4$

X_{Sr} vs t diagrams (Fig. 4) obtained by using four particle size fractions of celestite concentrate, 1 L solution obtained by dissolving 1.2 mol of $H_2C_2O_4$, 358 K and 500 r/min. As expected, the conversion reaction rate of $SrSO_4$ was increased with decreasing particle size. The number of particles increases by using the same amount of concentrated celestite with smaller particle size. Thus, surface area of the reacting solid particles increases. The topochemical reaction proceeds on the surfaces of $SrSO_4$ particles and therefore the fractional conversion obtained at the same reaction time is higher when celestite concentrate with smaller particle sizes was used.

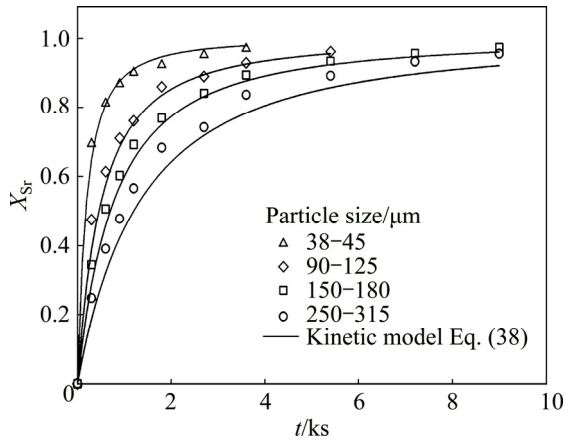

Fig. 4 X_{Sr} vs t diagrams for various particle sizes of celestite concentrate (celestite: 0.0104 mol, solution: 1 L, $H_2C_2O_4$: 1.2 mol, temperature: 358 K, stirring speed: 500 r/min)

3.7 Kinetics of conversion reaction of $SrSO_4$

The solubility product constant of $SrC_2O_4·H_2O$ at 298 K ($K_{sp,SrC_2O_4·H_2O}=5\times10^{-8}$) which is the intermediate product of conversion reaction of $SrSO_4$ to $H[Sr(C_2O_4)_{1.5}(H_2O)]$ is less than the solubility product constant of $SrSO_4$ ($K_{sp,SrSO_4}=2.8\times10^{-7}$) [22,31]. There is no information in literature about the solubility product constant of $Sr(HC_2O_4)(C_2O_4)_{0.5}·H_2O$. It is evident that the affinity of Sr^{2+} ions to $C_2O_4^{2-}$ ions is higher than that of SO_4^{2-} ions. This is the driving force for the conversion reaction.

In our previous study, we have proposed the conversion mechanism of $SrSO_4$ to $H[Sr(C_2O_4)_{1.5}(H_2O)]$ [27]. The shape of fractional conversion vs time diagrams shown in Figs. 2(a−e) supports the proposed mechanism. The conversion of $SrSO_4$ proceeds according to proposed mechanism as follows: $SrSO_4$ reacts with $H_2C_2O_4$ on the surfaces of particles and is converted according to irreversible Reaction (4a) to adsorbed $SrC_2O_4·H_2O$. At the same time, adsorbed $SrC_2O_4·H_2O$ dissolves rapidly in $H_2C_2O_4$ solution according to the equilibrium Reaction (4b) until saturation conditions are achieved. $C_2O_4^{2-}$ reacts with H^+ to form $HC_2O_4^-$ according to the equilibrium Reaction (4c). By achievement of the saturation concentration according to Reaction (4b), dense (non-porous) $SrC_2O_4·H_2O$ protective layer forms on the reactant particle surfaces according to Reaction (4a) at the end of the first step of conversion reaction. While Reaction (5) proceeds very slowly with respect to

Reactions (4a)−(4c), assuming that it has a negligible effect on the fractional conversion of $SrSO_4$ until the formation of a dense layer of $SrC_2O_4{\cdot}H_2O$. The dense layer of $SrC_2O_4{\cdot}H_2O$ hinders the collision between the $SrSO_4$ particle surfaces and $H_2C_2O_4$ molecules in the solution. Thus, the conversion reaction can no longer continue. In order to continue the reaction, adsorbed $SrC_2O_4{\cdot}H_2O$ must be reacted with $H_2C_2O_4$ to form on one hand water soluble $H[Sr(C_2O_4)_{1.5}(H_2O)]$ and on other hand new uncovered surfaces on the surfaces of unreacted $SrSO_4$ particles (equilibrium Reaction (5)). The shape of the fractional conversion vs time diagrams indicates that the rate of Reaction (5) depends on $H_2C_2O_4$ concentration. Reactions (4a) and (4b) proceed very fast and $SrC_2O_4{\cdot}H_2O$ is formed from $SrSO_4$ during the reactive dissolution of $SrC_2O_4{\cdot}H_2O$ with $H_2C_2O_4$ to form $H[Sr(C_2O_4)_{1.5}(H_2O)]$ according to Reaction (5). A protective layer of $SrC_2O_4{\cdot}H_2O$ forms around the surfaces of $SrSO_4$ particles by the achievement of the saturation concentration of $H[Sr(C_2O_4)_{1.5}(H_2O)]$ (Reaction (6)). At the same time, by the achievement of the saturation concentration of ($H[Sr(C_2O_4)_{1.5}(H_2O)]$) in the solution, equilibrium conditions dominate according to Reaction (5) which hinders the reaction to continue.

At low temperatures and $H_2C_2O_4$ concentrations, the approximately horizontal outgoing of the fractional conversion vs time diagrams (Figs. 2(a−e)) indicates that at longer reaction durations, approximately equilibrium and saturation conditions are achieved in the reaction media according to Reactions (5) and (6).

$$SrSO_4(s)+H_2C_2O_4(d)+H_2O(d)\longrightarrow SrC_2O_4{\cdot}H_2O(s)+H^+(aq)+HSO_4^-(aq) \quad (4a)$$

$$SrC_2O_4{\cdot}H_2O(s)\rightleftharpoons Sr^{2+}(aq)+C_2O_4^{2-}(aq)+H_2O(d) \quad (4b)$$

$$C_2O_4^{2-}(aq)+H^+(aq)\rightleftharpoons HC_2O_4^-(aq) \quad (4c)$$

$$SrC_2O_4{\cdot}H_2O(s)+0.5H_2C_2O_4(d)\rightleftharpoons H[Sr(C_2O_4)_{1.5}(H_2O)](d) \quad (5)$$

$$H[Sr(C_2O_4)_{1.5}(H_2O)](d)\rightleftharpoons Sr(HC_2O_4)(C_2O_4)_{0.5}{\cdot}H_2O(s) \quad (6)$$

The consumption of spherical $SrSO_4$ particles according to Reactions 4(a) and (4b) was explained by using the Shrinking Core Model proposed by LEVENSPIEL [32]. Equation (7) is derived according to this model which shows the relationship between X_S vs t where $k_1=2k_1'$:

$$1-(1-X_S)^{1/3}=\frac{k_1'C_{ox,0}^p}{\rho_s r_s}t=\frac{k_1C_{ox,0}^p}{\rho_s R_s}t=\frac{\psi}{\rho_s R_s}t=\omega t \quad (7)$$

By using X_S vs t data in Figs. 2(a−e) at initial stages of the conversion reaction of $SrSO_4$, linear diagrams were obtained by plotting $1-(1-X_S)^{1/3}$ vs t. From the slopes of these linear diagrams, ω values were calculated. ψ values were calculated by considering the density (ρ_s=21.56 kmol/m^3) and mean particle size (mean particle diameter) ($R_s=1.075\times10^{-4}$ m) of the celestite particles. ln ψ vs ln C_{ox} diagrams were drawn for each constant temperature (Fig. 5). From the slopes of these parallel straight lines, the order of $H_2C_2O_4$ concentration was calculated as p=0.33. Reaction rate constants (ln k_1) for each temperature were estimated from the intercepts of these parallel straight lines with the ordinate axis at ln $C_{ox,0}$=0. ln k_1 is given according to Arrhenius Equation (Eq. (8)). Diagram was drawn between ln k_1 and $1/T$ to calculate the kinetic parameters as pre-exponential factor (ln $k_{1,0}$) and apparent activation energy (E_1) (Fig. 6). E_1 and ln $k_{1,0}$ were calculated from the slope of the straight line and from the intercept of the straight line with the ordinate axis at $1/T$=0 (E_1=43 kJ/mol and $k_{1,0}$=3.21 (kmol·m^{-3})$^{0.67}$·m·s^{-1}.

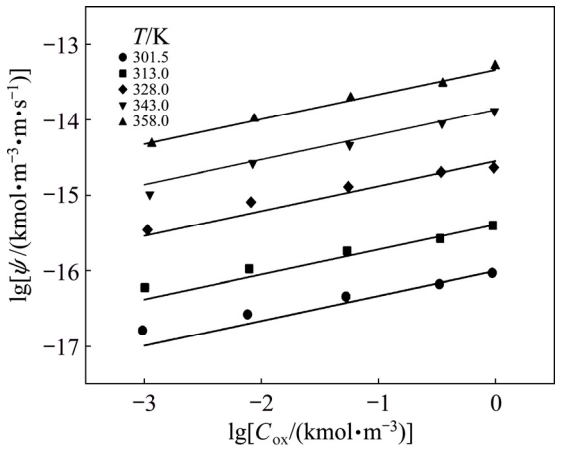

Fig. 5 ln ψ vs ln C_{ox} diagrams for Reaction (4a) at various temperatures (celestite: 0.0104 mol, particle size: 90−125 μm, solution: 1 L, $H_2C_2O_4$: 0.1, 0.2, 0.4, 0.8 and 1.2 mol, stirring speed: 500 r/min)

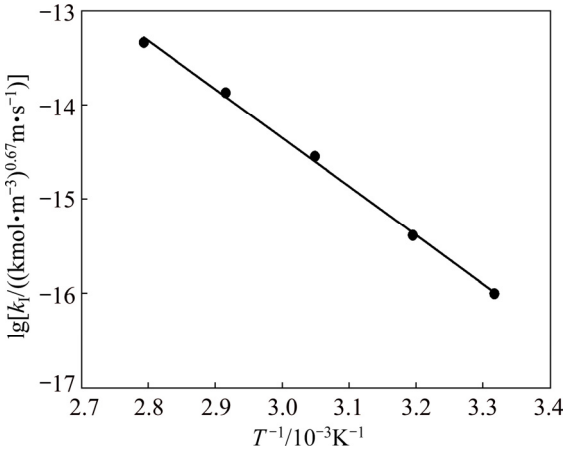

Fig. 6 Arrhenius plot of Reaction (4a) (celestite: 0.0104 mol, particle size: 90−125 μm, solution: 1 L, $H_2C_2O_4$: 0.1, 0.2, 0.4, 0.8, 1.2 mol, temperature: 301.5, 313, 328, 343, 358 K, stirring speed: 500 r/min)

$$\ln k_1 = \ln k_{1,0} - \frac{E_1}{RT} \quad (8)$$

Kinetic model Eq. (9), which is the rearranged form of Eq. (7), is obtained by using the known density, mean particle diameter of celestite particles, the calculated pre-exponential factor and apparent activation energy for the conversion reaction according to Reaction (4a). As can be seen from Kinetic Model Eq. (9), X_S is a function of temperature, $H_2C_2O_4$ concentration and time where R= 8.314 kJ·kmol^{-1}·K^{-1}. X_S vs t diagrams were plotted using Kinetic model Eq. (9) for each temperature and $H_2C_2O_4$ concentration and shown as solid lines in Figs. 2(a−e) for the initial times of Reactions (4a) and (4b):

$$X_S = 1 - \left[1 - \frac{3.21\exp(-43000/RT)C_{ox,0}^{0.33}}{21.56\times1.07\times10^{-4}}t\right]^3 \quad (9)$$

It can be seen that the agreement between the solid lines obtained according to the Kinetic model Eq. (9) and the experimental findings is good for the initial stage of conversion reaction of $SrSO_4$. After a certain fractional conversion, the experimental data lie below the line drawn according to Kinetic model Eq. (9). This is due to the formation of $SrC_2O_4·H_2O$ as a protective layer on the surfaces of $SrSO_4$ particles according to Reaction (4a) which hinders the extension of the conversion reaction. Covering of $SrSO_4$ particle surfaces with $SrC_2O_4·H_2O$ occurs when equilibrium conditions are achieved according to Reaction (4b). The conversion reaction continues with a slow dissolution rate of $SrC_2O_4·H_2O$ with $H_2C_2O_4$ according to equilibrium Reaction (5). SO_4 and Sr present in the $SrSO_4$ pass into the solution as HSO_4^- ions and $H[Sr(C_2O_4)_{1.5}(H_2O)]$ during the conversion reaction. If the conversion of $SrSO_4$ is calculated according to the S element in the HSO_4^- ion (X_S) and Sr element (X_{Sr}) in the $H[Sr(C_2O_4)_{1.5}(H_2O)]$, it was observed that $X_{Sr}<X_S$ (Figs. 2(a−e)). The difference between X_{Sr} and X_S is related to the formation of insoluble protective layer of $SrC_2O_4·H_2O$ on the surfaces of $SrSO_4$ particles. Reactions (4a), (4b) and (5) are written as a consecutive reaction considering the mechanism proposed by ZORAGA et al [27] and according to the observation that the dissolution is increased by increasing $H_2C_2O_4$ concentration. Therefore, firstly $SrC_2O_4·H_2O$ must be formed according to Reactions (4a) and (4b), and then this must be dissolved reactively with $H_2C_2O_4$ according to Reaction (5).

Another reaction mechanism which must be considered is the formation of solid $Sr(HC_2O_4)$-$(C_2O_4)_{0.5}·H_2O$ instead of $SrC_2O_4·H_2O$ in the first step as a protective layer around the surfaces of $SrSO_4$ particles during reaction of 1 mol $SrSO_4$ with 1.5 mol $H_2C_2O_4$ and in the second step the dissolution of this solid strontium chelate compound ($Sr(HC_2O_4)(C_2O_4)_{0.5}·H_2O$) to soluble strontium oxalate chelate compound ($H[Sr(C_2O_4)_{1.5}(H_2O)]$). In this case, if the formation rate of solid $Sr(HC_2O_4)(C_2O_4)_{0.5}·H_2O$ in the first step is higher than the non-reactive dissolution rate of $Sr(HC_2O_4)(C_2O_4)_{0.5}·H_2O$ to $H[Sr(C_2O_4)_{1.5}(H_2O)]$ in the second step, a dense layer of $Sr(HC_2O_4)(C_2O_4)_{0.5}·H_2O$ forms on the surfaces of the $SrSO_4$ particles and conversion reaction is controlled by the second step. This means that the reaction rate of the second step must be in zero order with respect to the $H_2C_2O_4$ because the non-reactive dissolution of a solid must be a zero order reaction. Since experimental results showed that the reaction rate of the second step is a function of $H_2C_2O_4$ concentration, this mechanism is not valid.

Reaction (5) is an equilibrium reaction, and its rate decreases progressively. When the concentration of $H[Sr(C_2O_4)_{1.5}(H_2O)]$ reaches the saturation concentration, it equals zero. The driving force for Reaction (5) is the difference between the saturation concentration and real concentration of $H[Sr(C_2O_4)_{1.5}(H_2O)]$ in the solution.

When Reaction (5) is the slowest step, its rate controls the conversion reaction. The reactive dissolution rate equation for the spherical $SrC_2O_4·H_2O$ layer was derived according to the Shrinking Core Model proposed by LEVENSPIEL [32], as given by Eq. (10), where $k_2=2k_2''$, $k_2'=2k_2'''$ and $v=v_{so}:v_{ox}$ =1:0.5=2.

$$\frac{1}{3(1-X_{Sr})^{2/3}}\frac{dX_{Sr}}{dt} = v\frac{k_2''}{\rho_s r_s}C_{ox}^q - \frac{k_2'''}{\rho_s r_s}C_{Ch} = 2\frac{k_2}{\rho_s R_s}C_{ox}^q - \frac{k_2'}{\rho_s R_s}C_{Ch} \quad (10)$$

By derivation of Eq. (10), it is assumed that the non-elementary reaction rate for the forward reaction is in the qth order with respect to the $H_2C_2O_4$ concentration and for the reverse reaction in the 1st order with respect to the $H[Sr(C_2O_4)_{1.5}(H_2O)]$ concentration. The use of X_{Sr} instead of X_S in Eq. (10) is based on the following experimental facts. Firstly, Sr is present both in solid state as $SrC_2O_4·H_2O$ and dissolved state as $H[Sr(C_2O_4)_{1.5}(H_2O)]$ in the solution and secondly, the concentration of $H[Sr(C_2O_4)_{1.5}(H_2O)]$ is used in the reaction rate equation.

Equation (11) is valid when equilibrium is achieved according to Reaction (5) and the conversion reaction interrupts under this condition:

$$2k_2C_{ox,e}^q = k_2'C_{Ch,e} \quad (11)$$

Equation (12) is obtained by replacement of k_2' in Eq. (10):

$$\frac{1}{3(1-X_{Sr})^{2/3}}\frac{dX_{Sr}}{dt} = \frac{2k_2C_{ox}^q}{\rho_s R_s}\left[1 - \frac{C_{Ch}}{2C_{ox}^q}\Big/\frac{C_{Ch,e}}{2C_{ox,e}^q}\right] \quad (12)$$

C_{Ch} varies during conversion reaction from zero to

$C_{Ch,e}$. The value of $C_{Ch,e}$ depends on the reaction temperature and amount of $H_2C_2O_4$ dissolved for the preparation of 1 L reactive solution. Because of the use of excess amounts of $H_2C_2O_4$ compared to the stoichiometric requirement for the complete conversion reaction of $SrSO_4$ (0.0104 mol), it is apparent that $C_{ox}\approx C_{ox,o}\approx C_{ox,e}$ is valid. This assumption brings negligible error but it makes easier the mathematical procedure to obtain the kinetic parameters. Equation (13) was obtained by applying this assumption to Eq. (12):

$$\frac{1}{(1-X_{Sr})^{2/3}}\frac{dX_{Sr}}{dt}=\frac{6k_2C_{ox}^q}{\rho_s R_s}\left[1-\frac{C_{Ch}}{2C_{Ch,e}}\right] \quad (13)$$

The following Eqs. (14)−(17) are derived by considering initial amount of $H_2C_2O_4$, initial amount of celestite, volume of solution, stoichiometric coefficients of substances in the conversion reaction and considering that at the second step after a certain $X_{Sr,i}$ value the rate of $SrC_2O_4\cdot H_2O$ dissolved according to Reaction (5) is equal to the rate of $SrC_2O_4\cdot H_2O$ formed according to Reaction (4a):

$$C_{Ch}=\frac{n_{s,0}}{V}X_{Sr} \quad (14)$$

$$C_{Ch,e}=\frac{n_{s,0}}{V}X_{Sr,e} \quad (15)$$

$$C_{ox}=C_{ox,0}-1.5\frac{n_{s,0}}{V}X_{Sr}\approx C_{ox,0} \quad (16)$$

$$C_{ox,e}=C_{ox,0}-1.5\frac{n_{s,0}}{V}X_{Sr,e}\approx C_{ox,0} \quad (17)$$

By replacement of the concentrations given in Eqs. (14)−(17) in Eq. (13) and by integration of the derived equation, Eq. (18) is obtained:

$$I=\int_0^{X_{Sr}}\frac{dX_{Sr}}{(1-X_{Sr})^{2/3}(1-\frac{X_{Sr}}{X_{Sr,e}})}=\frac{6k_2C_{ox,0}^q}{\rho_s R_s}\int_0^t dt=$$

$$\frac{6k_2C_{ox,0}^q}{\rho_s R_s}t=\frac{6\xi}{\rho_s R_s}t=\varphi t \quad (18)$$

Integration of Eq. (18) leads to Eq. (19), where α, β, γ, δ, ε, κ and λ can be expressed by Eqs. (20)−(26), where $0<X_{Sr,e}<1$:

$$I=\alpha\left\{\ln\frac{\beta/\gamma}{\delta/\varepsilon}-2\sqrt{3}[\tan^{-1}(\frac{\kappa}{\sqrt{3}})-\tan^{-1}(\frac{\lambda}{\sqrt{3}})]\right\}=\varphi t \quad (19)$$

$$\alpha=\frac{X_{Sr,e}}{2(X_{Sr,e}-1)^{2/3}} \quad (20)$$

$$\beta=(1-X_{Sr})^{2/3}-(X_{Sr,e}-1)^{1/3}(1-X_{Sr})^{1/3}+(X_{Sr,e}-1)^{2/3} \quad (21)$$

$$\gamma=[(1-X_{Sr})^{1/3}+(X_{Sr,e}-1)^{1/3}]^2 \quad (22)$$

$$\delta=1-(X_{Sr,e}-1)^{1/3}+(X_{Sr,e}-1)^{2/3} \quad (23)$$

$$\varepsilon=[1+(X_{Sr,e}-1)^{1/3}]^2 \quad (24)$$

$$\kappa=\frac{2(1-X_{Sr})^{1/3}}{(X_{Sr,e}-1)^{1/3}}-1 \quad (25)$$

$$\lambda=\frac{2}{(X_{Sr,e}-1)^{1/3}}-1 \quad (26)$$

Using appropriate values of $X_{Sr,e}$, the graphical representation of I vs t according to Eq. (19) must give a straight line which begins from the origin of the graph and has a slope of φ. Appropriate $X_{Sr,e}$ values which gave straight lines for each temperature and $H_2C_2O_4$ concentration were determined. Figure 7 shows the straight lines obtained at 328 K using 1 L solution which was obtained by dissolving 0.1, 0.2, 0.4, 0.8 and 1.2 mol $H_2C_2O_4$. Diagrams drawn for other temperatures and same mole amounts of $H_2C_2O_4$ were not shown to avoid repetition.

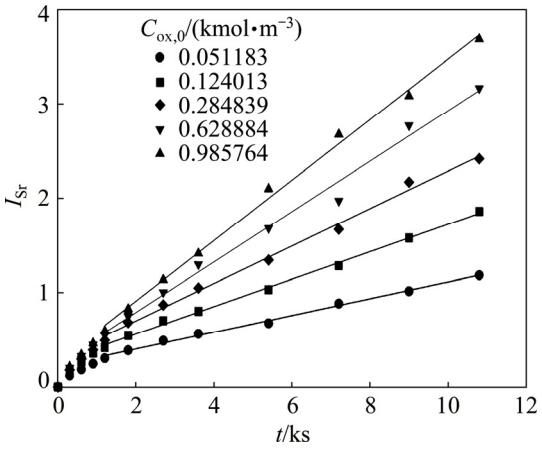

Fig. 7 I_{Sr} vs t diagrams for Reaction (5) (celestite: 0.0104 mol, particle size: 90−125 μm, solution: 1 L, $H_2C_2O_4$: 0.1, 0.2, 0.4, 0.8, 1.2 mol, temperature: 328 K, stirring speed: 500 r/min)

For obtaining straight lines that start from the origin of the graph, Reactions (4a) and (4b) must take place rapidly forming a thin layer of $SrC_2O_4\cdot H_2O$ and Reaction (5) must be continued slowly until equilibrium conditions. Reactions (4a) and (4b) (fast) and Reaction (5) (slow) take place forming a thin protective layer on the surfaces of shrinking $SrSO_4$ particles until a $X_{Sr,i}$ value and after this value Reaction (5) continues slowly and controls the overall rate of the reaction. This is the reason why I vs t straight lines did not start from the origin of the graph. Therefore, linear relationship is obtained only after certain $X_{Sr,i}$ value (Fig. 7) and this linear relationship is given as Eq. (27). φ and I_0 are calculated from the slope of this straight line and from

the intercept of this straight line with the ordinate axis at t=0:

$$I=I_0+\varphi t \tag{27}$$

φ and I_0 were calculated by plotting I vs t diagrams using experimental data. ξ values were calculated from Eq. (19) using the known density, mean particle diameter of $SrSO_4$ for each constant temperature and various $H_2C_2O_4$ concentrations. ln ξ vs ln $C_{ox,0}$ diagrams were drawn for each constant temperature (Fig. 8) and from the slopes of each straight line and from the intercepts of these straight lines at ln $C_{ox,0}$=0, reaction order, q, with respect to the $H_2C_2O_4$ concentration (Table 4) and ln k_2 was calculated. E_2 and ln $k_{2,0}$ were calculated for the forward Reaction (5) from the slope and the intercept of the straight line at 1/T=0 from the Arrhenius plot of k_2 (Fig. 9) as 32.74 kJ/mol and 1.92×10^{-2} $(kmol\cdot m^{-3})^{1-q}\cdot m\cdot s^{-1}$ ($k_{2,0}$), respectively (Eqs. (28) and (29)).

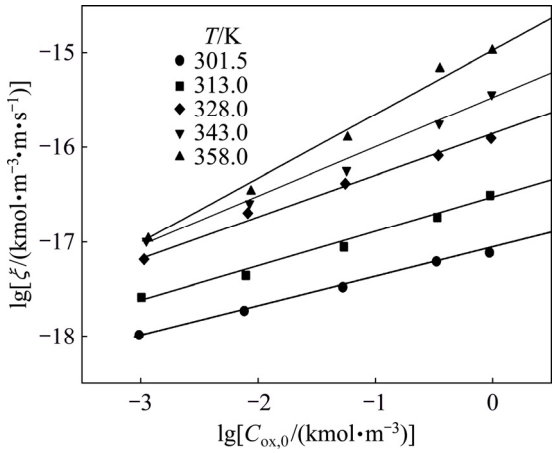

Fig. 8 ln ξ vs ln $C_{ox,0}$ diagrams for Reaction (5) at various temperatures (celestite: 0.0104 mol, particle size: 90−125 μm, solution: 1 L, $H_2C_2O_4$: 0.1, 0.2, 0.4, 0.8, 1.2 mol, stirring speed: 500 r/min)

Table 4 Orders of $H_2C_2O_4$ concentration in rate equation for forward Reaction (5) (celestite: 0.0104 mol, particle size: 90−125 μm, $H_2C_2O_4$: 0.1, 0.2, 0.4, 0.8, 1.2 mol, solution: 1 L, stirring speed: 500 r/min)

Temperature/K	301.5	313	328	343	358
q	0.31	0.36	0.44	0.52	0.68

$$k_2=k_{2,0}\exp(-\frac{E_2}{RT})=1.92\times10^{-2}\exp\left(-\frac{32740}{RT}\right) \tag{28}$$

$$\varphi=\frac{6k_2C_{ox,0}^q}{\rho_s R_s}=\frac{6\times1.92\times10^{-2}\exp(-\frac{32740}{RT})C_{ox,0}^q}{21.56\times1.075\times10^{-4}} \tag{29}$$

Appropriate $X_{Sr,e}$ value that gives linear relationship between I and t was determined using experimental results obtained at constant temperature and $H_2C_2O_4$ concentration. $X_{Sr,0}$ was calculated using this appropriate $X_{Sr,e}$ value in Eq. (19) and taking I=I_0. In Eq. (19), α, β, γ and κ remain unchanged but δ, ε and λ change according to the Eqs. (30)−(32), respectively, for the boundary conditions of X_{Sr}=$X_{Sr,0}$ at t=0 and X_{Sr}=X_{Sr} at t:

$$\delta'=(1-X_{Sr,0})^{2/3}-(X_{Sr,e}-1)^{1/3}(1-X_{Sr,0})^{1/3}+(X_{Sr,e}-1)^{2/3} \tag{30}$$

$$\varepsilon'=[(1-X_{Sr,0})^{1/3}+(X_{Sr,e}-1)^{1/3}]^2 \tag{31}$$

$$\lambda'=\frac{2(1-X_{Sr,0})^{1/3}}{(X_{Sr,e}-1)^{1/3}}-1 \tag{32}$$

α, β, γ, κ, δ', ε' and λ' given as Eqs. (20)−(22), (25) and (30)−(32) were calculated for each X_{Sr} using $X_{Sr,0}$ and $X_{Sr,e}$. I was estimated by using calculated α, β, γ, κ, δ', ε' and λ' values. Calculated X_{Sr} vs t diagrams starting from $X_{Sr,i}$ were shown as solid lines in Figs. 2(a−e) together with the experimental findings.

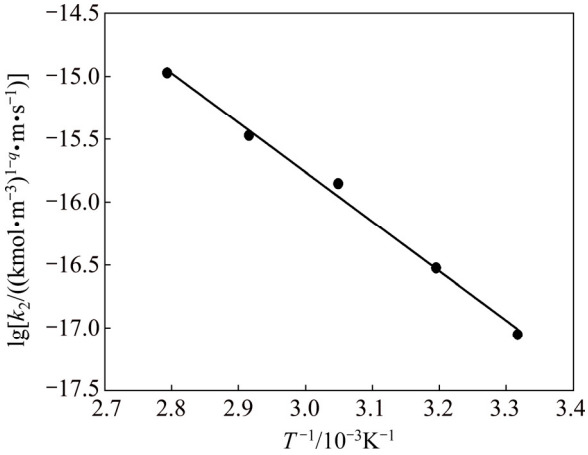

Fig. 9 Arrhenius plot of forward Reaction (5) (celestite: 0.0104 mol, particle size: 90−125 μm, solution: 1 L, $H_2C_2O_4$: 0.1, 0.2, 0.4, 0.8, 1.2 mol, temperature: 301.5, 313, 328, 343, 358 K, $H_2C_2O_4$: 1.2 mol, stirring speed: 500 r/min)

It was observed that there is a good agreement between experimental results and the results obtained from the Kinetic model Eq. (27) for X_{Sr} higher than $X_{Sr,i}$ except for the experiment that was carried out at 358 K using 1 L solution obtained by dissolving 1.2 mol $H_2C_2O_4$ (particular case). This particular case was discussed below together with the results that was obtained using various sizes of celestite particles and the same experimental conditions.

$Sr(HC_2O_4)(C_2O_4)_{0.5}\cdot H_2O$ must crystallize in the solution when concentration of $H[Sr(C_2O_4)_{1.5}(H_2O)]$ reaches the saturation. In this case, X_{sr} must not be changed. But contrary to this, X_S must increase during the extent of reaction. A phenomenon like this cannot be seen in the X_{Sr} vs t and X_S vs t results given in

Figs. 2(a−e). In contrary, $Sr(HC_2O_4)(C_2O_4)_{0.5}\cdot H_2O$ must crystallize on the surfaces of celestite particles.

Equilibrium constant of Reaction (5) (K_2) was calculated for each temperature by Eq. (33) using appropriate $C_{Ch,e}$ value which provides the linearity of the I vs t diagram and $C_{ox,0}$ value given in Table 3. The average K_2 was calculated by taking the arithmetic mean of the K_2 obtained at the same temperature:

$$K_2=\frac{k_2}{k_2'}=\frac{C_{Ch,e}}{2C_{ox,e}^q} \tag{33}$$

The rate constant (k_2') of reverse Reaction (5) for each temperature was calculated using the average K_2 and k_2 values calculated from Eq. (28). $\ln k_2'$ vs $1/T$ diagram was plotted (Fig. 10) and E_2' and $\ln k_{2,0}'$ were calculated from the slope of the straight line and the intercept of the straight line with the ordinate axis at $1/T$=0. The calculated values of E_2' (10.04 kJ/mol) and $k_{2,0}'$ (1.0×10^{-3} m/s) were given in the Arrhenius type equation of k_2' (Eq. (34)):

$$k_2'=1.0\times10^{-3}\exp\left(-\frac{10040}{RT}\right) \tag{34}$$

The relationship between the heat of reaction and activation energies for the forward and reverse Reaction (5) is given by

$$\Delta H^0=E_2-E_2'=2.27\ \text{kJ/mol} \tag{35}$$

Since Reaction (5) is endothermic, it extends to the right side by increasing temperature in accordance with Le Chatelier's Principle. This finding is in good agreement with the experimental results.

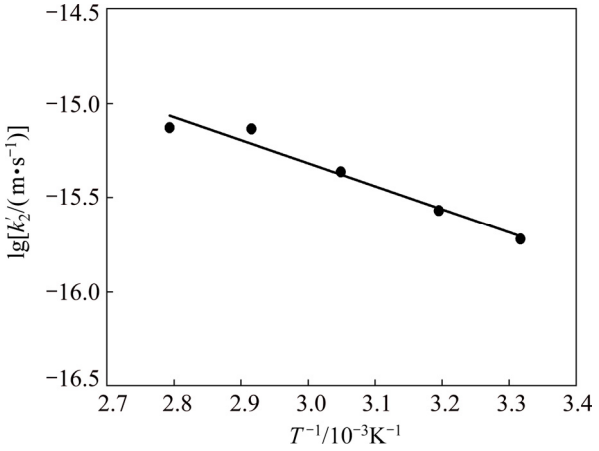

Fig. 10 Arrhenius plot of reverse Reaction (5) (k_2') (celestite: 0.0104 mol, particle size: 90−1250 μm, solution: 1 L, $H_2C_2O_4$: 0.1, 0.2, 0.4, 0.8, 1.2 mol, temperature: 301.5, 313, 328, 343, 358 K, stirring speed: 500 r/min)

3.8 Kinetics for particular case

It was determined that the conversion reaction is completed when 2 g various particle sizes of celestite concentrate, 1 L solution obtained by dissolving 1.2 mol $H_2C_2O_4$, 358 K and 500 r/min were used (Fig. (4)). According to this finding, $X_{Sr,e}$ in Eq. (18) can be taken as 1 and Eq. (36) can be derived where v=2. Equation (37) was obtained by integration of Eq. (36):

$$\int_0^{X_{Sr}}\frac{dX_{Sr}}{(1-X_{Sr})^{5/3}}=\frac{3vk_2C_{ox,0}^q}{\rho_s R_s}t=\frac{3v\xi}{\rho_s R_s}t=\varphi t \tag{36}$$

$$(1-X_{Sr})^{-2/3}-1=\frac{2vk_2C_{ox,0}^q}{\rho_s R_s}t=\chi t \tag{37}$$

$(1-X_{Sr})^{-2/3}-1$ vs t diagram was plotted (Fig. 11). Straight lines obtained for each particle size indicate that the Kinetic model Eq. (37) is in good agreement with the experimental findings.

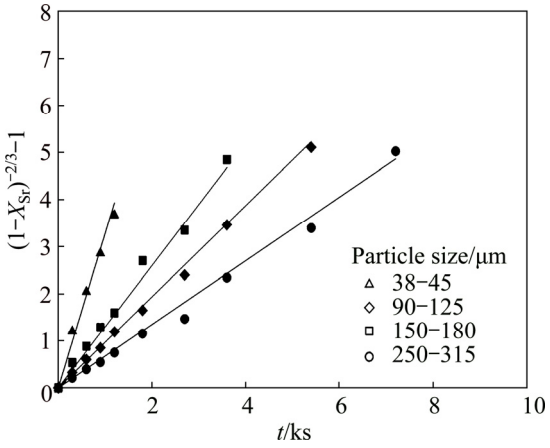

Fig. 11 $(1-X_{Sr})^{-2/3}-1$ vs t diagrams for various particle sizes of celestite concentrate (celestite: 0.0104 mol, solution: 1 L, $H_2C_2O_4$: 1.2 mol, temperature: 358 K, stirring speed: 500 r/min)

The slope of each line in Fig. 11 gives χ values which is inversely proportional to average particle diameter (R_s). R_s was calculated by taking the arithmetic mean of each fraction and diagram was drawn between χ and $1/R_s$ (Fig. 12). Straight line obtained in Fig. 12 indicates that the slope of the straight line is inversely proportional to R_s and therefore the reaction rate is under chemical reaction control. Additionally, it can be said that forward Reaction (5) is effective and reverse Reaction (5) is negligible under the reaction conditions applied.

The rate constant of forward Reaction (5) (k_2) was calculated from the slope value (χ) to be 7.48×10^{-7} $(\text{kmol}\cdot\text{m}^{-3})^{1-q}\cdot\text{m}\cdot\text{s}^{-1}$ by taking q=0.68 and v=2. The value of 7.48×10^{-7} is 2.33 times the value of 3.21×10^{-7} calculated using Eq. (28). This finding reveals that the chemical reaction obtained at 358 K and 1 L solution obtained by dissolving 1.2 mol $H_2C_2O_4$ is different from the chemical reaction that takes place under other experimental conditions used in this study.

According to this finding, stoichiometric coefficient ratio (v) in Reaction (5) must be $v=v_{so}:v_{ox}=4.65$ instead of 2. KNAEPEN et al [25] proposed solid strontium chelate compounds with various chemical formulas such as $SrC_2O_4(H_2C_2O_4)_{0.5}\cdot H_2O$, $SrC_2O_4(H_2C_2O_4)_{0.43}\cdot 1.2H_2O$ and $SrC_2O_4(H_2C_2O_4)_{0.09}\cdot 1.7H_2O$. The chemical formula of soluble acidic strontium chelate compound that formed using 2 g of various particle size celestite, 1 L solution obtained by dissolving 1.2 mol $H_2C_2O_4$, 358 K and 500 r/min can be written as $H_{0.430}[Sr(C_2O_4)_{1.215}\cdot x(H_2O)]$ according to the experimental findings.

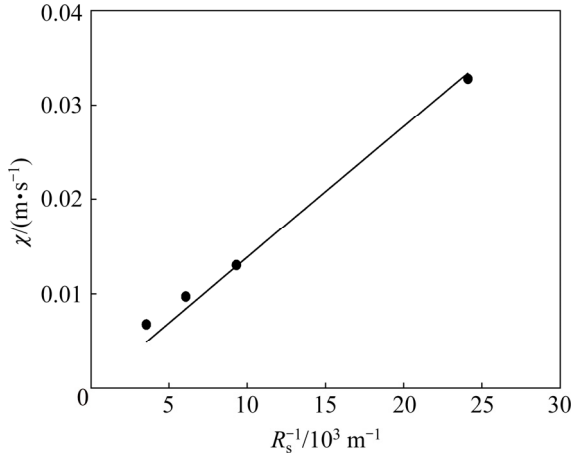

Fig. 12 χ vs $1/R_s$ diagram for various particle sizes of celestite concentrate (celestite: 0.0104 mol, solution: 1 L, $H_2C_2O_4$: 1.2 mol, temperature: 358 K, stirring speed: 500 r/min)

Equation (37) can be rearranged to Kinetic Model Eq. (38) using ρ_s=21.56 kmol/m^3, 358 K, $k_2=7.48\times10^{-7}$ (kmol·m^{-3})$^{0.32}$·m·s^{-1} and v=2. Solid lines obtained using kinetic model Eq. (38) (Fig. 4) are in good agreement with the experimental findings.

$$X_{Sr}=1-\left(1+\frac{1.385\times10^{-7}}{R_s}t\right)^{-3/2} \tag{38}$$

A similar equation with Eq. (37) can be derived by assuming that Reactions (4a) and (4b) proceed more rapidly than Reaction (5), Reaction (5) is irreversible and rate of Reaction (5) is in the first order with respect to the celestite concentration and in the qth order with respect to the $H_2C_2O_4$ concentration (The use of solid reactant concentration is not a preferred method in the derivation of rate equation for a heterogeneous type reaction). Equation (39) was derived using the above mentioned assumptions and shrinking core model. Equation (40) was obtained by rearrangement of Eq. (39). Integration of Eq. (40) gives Eq. (41) which is similar with Eq. (37), where χ' differs from χ only by containing the initial concentration of celestite particles ($C_{s,0}$) and $2k_2'=k_2$:

$$\frac{1}{3(1-X_{Sr})^{2/3}}\frac{dX_{Sr}}{dt}=\frac{vk_2'C_sC_{ox}^q}{\rho_s r_s}=\frac{vk_2C_{s,0}(1-X_{Sr})C_{ox}^q}{\rho_s r_s} \tag{39}$$

$$\frac{dX_{Sr}}{(1-X_{Sr})^{5/3}}=\frac{3vk_2C_{s,0}C_{ox}^q}{\rho_s R_s}dt \tag{40}$$

$$(1-X_{Sr})^{-2/3}-1=\frac{2vk_2C_{s,0}C_{ox,0}^q}{\rho_s R_s}t=\chi' t \tag{41}$$

Equation (41) is valid only for the particular case (2 g celestite concentrate with various particle sizes, 1 L solution obtained by dissolving 1.2 mol $H_2C_2O_4$, 358 K and 500 r/min).

4 Conclusions

(1) Conversion of $SrSO_4$ to $H[Sr(C_2O_4)_{1.5}(H_2O)]$ in aqueous $H_2C_2O_4$ solutions takes place as a consecutive reaction. In the first step, $SrC_2O_4\cdot H_2O$ is formed (Reaction (4a)). In the second step, $SrC_2O_4\cdot H_2O$ reacts with $H_2C_2O_4$ to form $H[Sr(C_2O_4)_{1.5}(H_2O)]$ (Reaction (5)). $Sr(HC_2O_4)(C_2O_4)_{0.5}\cdot H_2O$ crystallizes during cooling of the reaction mixture to room temperature when the solution reaches the saturation concentration of $H[Sr(C_2O_4)_{1.5}(H_2O)]$ (Reaction (6)).

(2) The reaction rate increases at the initial time of reaction by increasing the temperature using solutions with approximately same $H_2C_2O_4$ concentrations. This finding supports that the reaction rate is under chemical reaction kinetics control with definite apparent activation energy.

(3) The reaction extends very slowly after a certain time and ends by forming a protective layer of $SrC_2O_4\cdot H_2O$ around the surfaces of solid particles using solutions with low $H_2C_2O_4$ concentration at low constant temperature. Low conversions were obtained by reaching saturation concentration of $H[Sr(C_2O_4)_{1.5}(H_2O)]$.

(4) Conversion of $SrSO_4$ was increased by increasing concentration of $H_2C_2O_4$ at constant temperature. Therefore, it was found that conversion reaction rate of $SrSO_4$ is a function of the concentration of $H_2C_2O_4$. The reaction extends to higher saturation concentrations of $H[Sr(C_2O_4)_{1.5}(H_2O)]$ by using solutions with higher concentrations of $H_2C_2O_4$. $SrSO_4$ is converted totally to $H[Sr(C_2O_4)_{1.5}(H_2O)]$ using 358 K, 1 L solution obtained by dissolving 1.2 mol $H_2C_2O_4$ and 500 r/min.

(5) Decrease in the size of celestite particles increases the number and surface area of particles when same amount of celestite is used. Therefore, higher conversions were obtained by using the same reaction conditions with less particle size.

(6) The conversion reaction proceeds according to

shrinking core model until a protective layer of $SrC_2O_4·H_2O$ forms around the surfaces of celestite particles because of the solubility of $SrC_2O_4·H_2O$ in solutions containing $H_2C_2O_4$. In this case, X_S vs t relationship was given as Eq. (9), which includes kinetic parameters such as pre-exponential factor, apparent activation energy and order of $H_2C_2O_4$ concentration as 3.21 $(kmol·m^{-3})^{0.67}·m·s^{-1}$, 43 kJ/mol and 0.33, respectively.

(7) When the reversible reaction of $SrC_2O_4·H_2O$ with $H_2C_2O_4$ to form $H[Sr(C_2O_4)_{1.5}(H_2O)]$ is the slowest step, X_{Sr} vs t relationship can be derived as Eq. (19). In this equation, pre-exponential factor, apparent activation energy and order of $H_2C_2O_4$ concentration were determined to be $1.92×10^{-2}$ $(kmol·m^{-3})^{1-q}·m·s^{-1}$, 32.74 kJ/mol and 0.31−0.68, respectively.

(8) The conversion reaction was completed by using 358 K, 1 L solution obtained by dissolving 1.2 mol $H_2C_2O_4$ and different sizes of celestite particles. In this particular case, Reaction (5) is the slowest step and the fractional conversion vs time equation is derived as Eq. (38). In this equation, the reaction rate constant k_2 was determined as $7.48×10^{-7}$ $(kmol·m^{-3})^{0.32}·m·s^{-1}$. For this particular case, acidic strontium chelate with the chemical formula of $H_{0.430}[Sr(C_2O_4)_{1.215}(H_2O)]$ forms instead of $H[Sr(C_2O_4)_{1.5}(H_2O)]$.

Acknowledgments

The authors gratefully acknowledge the financial support of the Scientific Research Projects Coordination Unit of Istanbul University (Project number: 17344 and 31088)

Nomenclatures

aq	Aqueous
C_{Ch}	Concentration of chelate compound at time t
$C_{Ch,e}$	Equilibrium concentration of chelate compound
C_{ox}	$H_2C_2O_4$ concentration at time t
$C_{ox,e}$	$H_2C_2O_4$ equilibrium concentration
$C_{ox,0}$	$H_2C_2O_4$ initial concentration
C_s	$SrSO_4$ concentration at time t
$C_{s,0}$	$SrSO_4$ initial concentration
d	Dissolved
E_1	Activation energy of Reaction (6)
E_2	Activation energy of forward Reaction (7)
E_2'	Activation energy of reverse Reaction (7)
K_1	Equilibrium constant of Reaction (1)
K_2	Equilibrium constant of Reaction (2)
k_1, k_1'	Rate constants of Reaction (6)
$k_{1,0}$	Pre-exponential factor of Reaction (6) rate constant
k_2, k''_2	Rate constants of forward Reaction (7)
$k_{2,0}$	Pre-exponential factor of forward Reaction (7) rate constant
k_2', k'''_2	Rate constants of reverse Reaction (7)
$k'_{2,0}$	Pre-exponential factor of reverse Reaction (7) rate constant
$K_{Sp,i}$	Solubility product constant of compound i
$n_{s,0}$	Initial mol amount of $SrSO_4$
p, q	Order of $H_2C_2O_4$ concentration
r_s	Mean radius of $SrSO_4$ particles
R	Gas constant
R_s	Mean diameter of $SrSO_4$ particles
S	Solid
t	Time
T	Temperature
V	Volume of solution
X_i	Fractional conversion of i element in $SrSO_4$ to form soluble HSO_4^- or soluble chelate compound
X_S	Fractional conversion of S in $SrSO_4$ to form soluble HSO_4^-
X_{Sr}	Fractional conversion of Sr in $SrSO_4$ to form soluble chelate compound
$X_{Sr,e}$	Equilibrium fractional conversion of Sr in $SrSO_4$ to form soluble chelate compound
w_i	Mole amount of i element in $SrSO_4$ to form soluble HSO_4^- or soluble chelate compound
$w_{i,0}$	Initial mole amount of i element in $SrSO_4$ (i: S or Sr)
ΔH^0	Standard enthalpy of Reaction (7)
v_{so}	Stoichiometric coefficient of $SrC_2O_4·H_2O$ in Reaction (7)
v_{ox}	Stoichiometric coefficient of $H_2C_2O_4·H_2O$ in Reaction (7)
ρ_s	Density of $SrSO_4$

References

[1] KOBE A K, DEIGLMEIER N J. Conversion from strontium sulfate by metathesis with alkali carbonate solution [J]. Industrial and Engineering Chemistry, 1943, 35: 323−325.

[2] ERDEMOGLU M, CANBAZOGLU M. The leaching of SrS with water and the precipitation of $SrCO_3$ from leach solution by different carbonating agents [J]. Hydrometallurgy, 1998, 49: 135−150.

[3] OWUSU G, LITZ J E. Water leaching of SrS and precipitation of $SrCO_3$ using carbon dioxide as the precipitating agent [J]. Hydrometallurgy, 2000, 57: 23−29.

[4] SETEOUDEH N, WELHAM N J. Ball milling induced reduction of $SrSO_4$ by Al [J]. International Journal of Mineral Processing, 2011, 98: 214−218.

[5] SETEOUDEH N, WELHAM N J. Ball milling induced reduction of $SrSO_4$ by Mg [J]. International Journal of Mineral Processing, 2012, 104: 49−52.

[6] CHIANG J S, GOLDSTEIN D. Preparation of strontium carbonate [P]. US Patent: 4421729, 1983−12−20.
[7] de BUDA F. Method for recovery and conversion of strontium sulfate to strontium carbonate from low to medium grade celestite ores [P]. US Patent: 4666688, 1987−05−19.
[8] IWAI M, TOGURI J M. The leaching of celestite in sodium carbonate solution [J]. Hydrometallurgy, 1989, 22: 87−100.
[9] CASTILLEJOS A H, de la CRUZ DEL B, URIBE S. The direct conversion of celestite to strontium carbonate in sodium carbonate aqueous media [J]. Hydrometallurgy, 1996, 40: 207−222.
[10] ZORAGA M, KAHRUMAN C. Kinetics of conversion of celestite to strontium carbonate in solutions containing carbonate, bicarbonate and ammonium ions, and dissolved ammonia [J]. Journal of the Serbian Chemical Society, 2014, 79: 345−359.
[11] OBUT A, BALAZ P, GIRGIN I. Direct mechanochemical conversion of celestite to $SrCO_3$ [J]. Mineral Engineering, 2006, 19: 1185−1190.
[12] ERDEMOGLU M, AYDOGAN S, CANBAZOGLU M. A kinetic study on the conversion of celestite ($SrSO_4$) to $SrCO_3$ by mechanochemical processing [J]. Hydrometallurgy, 2007, 86: 1−5.
[13] SETEOUDEH N, WELHAM N J, AZAMI S M. Dry mechanochemical conversion of $SrSO_4$ to $SrCO_3$ [J]. Journal of Alloys and Compounds, 2010, 492: 389−391.
[14] BINGOL D, AYDOGAN S, BOZBAS S K. Optimization of the wet mechanochemical process conditions of $SrSO_4$ to $SrCO_3$ and $(NH_4)_2SO_4$ by using response surface methodology [J]. Metallurgical and Materials Transactions B, 2012, 43B: 1214−1219.
[15] BINGOL D, AYDOGAN S, BOZBAS S K. Production of $SrCO_3$ and $(NH_4)_2SO_4$ by dry mechanochemical processing of celestite [J]. Journal of Industrial and Engineering Chemistry, 2012, 18(2): 834−838.
[16] KNAEPEN E, VAN BAEL M K, SCHILDERMANS I, NOUWEN R, D'HAEN J, D'OLIESLAEGER M, QUAEYHAEGENS C, FRANCO D, YPERMAN J, MULLENS J, van POUCKE L C. Preparation and characterization of coprecipitates and mechanical mixtures of calcium - strontium oxalates using XRD, SEM-EDX and TG [J]. Thermochimica Acta, 1998, 318: 143−153.
[17] DOLLIMORE D. The thermal analysis of strontium oxalate [J]. Thermochimica Acta, 1985, 92: 543−546.
[18] VANHOYLAND G, BOURÉE F, VAN BAEL M K, MULLENS J, VAN POUCKE L C. Structure determination and refinement of acid strontium oxalate from X-ray and neutron powder diffraction [J]. Journal of Solid State Chemistry, 2001, 157 (2): 283−288.
[19] ZHANG Dong-bai, QI Li-min, MA Ji-ming, CHENG Hui-min. Biomimetic growth of strontium oxalate aggregates with unusual morphologies in the presence of poly(methacrylic acid) [J]. CrystEngComm, 2002, 4(88): 536−538.
[20] YU J, TANG H, CHENG B. Morphological control of strontium oxalate particles by PSMA−Mediated precipitation reaction [J]. Materials Chemistry and Physics, 2005, 91: 134−139.
[21] DALAL P V, SARAF K B. Growth of strontium oxalate crystals in agar−Agar gel [J]. Bulletin of Materials Science, 2011, 34(2): 377−381.
[22] OBUT A. Interaction of celestine concentrate and reagent grade $SrSO_4$ with oxalate solutions [J]. Acta Montanistica Slovaca, 2012, 17: 126−131.
[23] BACCE E D, PIRES A M, DAVALOS M R, JAFELICCI M Jr. Thermal decomposition and rehydration of strontium oxalate: Morphological evolution [J]. International Journal of Inorganic Materials, 2001, 3: 443−452.
[24] SELIM S A, ABD-EL-KHALIK M, RODRIQUE L. Thermal decomposition of strontium oxalate—Effect of various atmospheres [J]. Powder Technology, 1978, 20: 53−59.
[25] KNAEPEN E, MULLENS J, YPERMAN J, VAN POUCKE L C. Preparation and thermal decomposition of various forms of strontium oxalate [J]. Thermochimica Acta, 1996, 284: 213−227.
[26] AL-NEWAISER F A, AL-THABAITI S A, AL-YOUBI A O, OBAID A Y, GABAL, M A. Thermal decomposition kinetics of strontium oxalate [J]. Chemical Paper, 2007, 61(5): 370−375.
[27] ZORAGA M, KAHRUMAN C, YUSUFOGLU I. Determination of conversion reaction mechanism of celestite to acid strontium oxalate hydrate in aqueous solution of $H_2C_2O_4$ [J]. Hydrometallurgy, 2017, 171: 53−60.
[28] FURMAN N H. Scott's standard methods of chemical analysis [M]. 6th ed. New Jersey: David Van Nostrand Company, 1962.
[29] CAI W J, WANG Y. The chemistry, fluxes, and sources of carbon dioxide in the estuarine waters of the Satilla and Altamaha Rivers, Georgia [J]. Limnology and Oceanography, 1998, 43: 657−668.
[30] GOLDBERG R N, KISHORE N, LENNEN R M. Thermodynamic quantities for the ionization reactions of buffers [J]. Journal of Physical and Chemical Reference Data, 2002, 31 (2): 231−370.
[31] MONNIN C. A thermodynamic model for the solubility of barite and celestite in electrolyte solutions and seawater to 200 °C and to 1 kbar [J]. Chemical Geology,1999, 153: 187−209.
[32] LEVENSPIEL O. Chemical reaction engineering [M]. 3rd ed. New York: John Wiley & Sons Inc, 1999.

草酸水溶液中天青石转化为酸性草酸锶水合物的动力学

Mert ZORAGA, Cem KAHRUMAN, Ibrahim YUSUFOGLU

Istanbul University-Cerrahpasa, Engineering Faculty,
Metallurgical and Materials Engineering Department, 34320, Avcilar, Istanbul, Turkey

摘　要： $H_2C_2O_4$ 水溶液中 $SrSO_4$ 转化为酸性草酸锶水合物($H[Sr(C_2O_4)_{1.5}(H_2O)]$)的反应为连串反应。在连串反应的第一步，$SrSO_4$ 与 $H_2C_2O_4$ 反应，转化为赝晶 $SrC_2O_4{\cdot}H_2O$。第二步，$SrC_2O_4{\cdot}H_2O$ 与 $H_2C_2O_4$ 反应，生成 $H[Sr(C_2O_4)_{1.5}(H_2O)]$。如果溶液达到 $H[Sr(C_2O_4)_{1.5}(H_2O)]$ 的饱和浓度，当反应混合物冷却至室温时，$Sr(HC_2O_4)(C_2O_4)_{0.5}{\cdot}H_2O$ 发生结晶。根据溶解的 S 和 Sr 的量计算 $SrSO_4$ 的转化率发现，对于 $H_2C_2O_4$ 浓度大致相同的溶液，反应初始阶段的反应速率随着温度的升高而增大；在低 $H_2C_2O_4$ 浓度溶液中，一定时间之后反应进行缓慢，并且由于固体颗粒表面形成 $SrC_2O_4{\cdot}H_2O$ 保护层而停止；在一定温度下，$SrSO_4$ 的转化率随着 $H_2C_2O_4$ 浓度的增加而增大。利用收缩核模型得到每一步骤的动力学方程。

关键词： 天青石精矿；赝晶转化；速率方程；动力学参数；转化反应

(Edited by Bing YANG)